

Correlation between Cerebral Hemodynamic and Perfusion Pressure Changes in Non-Human Primates

A. Ruesch^a, MA. Smith^b, G. Wollstein^c, IA. Sigal^b, S. Nelson^b, JM. Kainerstorfer*^a

^aDepartment of Biomedical Engineering, Carnegie Mellon University, 5000 Forbes Avenue, Pittsburgh, PA 15213; ^b Department of Ophthalmology, University of Pittsburgh, Eye and Ear Institute, 203 Lothrop Street, Pittsburgh, PA 15213; ^c NYU Langone Eye Center, New York University School of Medicine, 462 First Avenue, New York, NY 10016

ABSTRACT

The mechanism that maintains a stable blood flow in the brain despite changes in cerebral perfusion pressure (CPP), and therefore guaranties a constant supply of oxygen and nutrients to the neurons, is known as cerebral autoregulation (CA). In a certain range of CPP, blood flow is mediated by a vasomotor adjustment in vascular resistance through dilation of blood vessels. CA is known to be impaired in diseases like traumatic brain injury, Parkinson's disease, stroke, hydrocephalus and others. If CA is impaired, blood flow and pressure changes are coupled and the oxygen supply might be unstable. Lassen's blood flow autoregulation curve describes this mechanism, where a plateau of stable blood flow in a specific range of CPP corresponds to intact autoregulation. Knowing the limits of this plateau and maintaining CPP within these limits can improve patient outcome. Since CPP is influenced by both intracranial pressure and arterial blood pressure, long term changes in either can lead to autoregulation impairment. Non-invasive methods for monitoring blood flow autoregulation are therefore needed. We propose to use Near infrared spectroscopy (NIRS) to fill this need. NIRS is an optical technique, which measures microvascular changes in cerebral hemoglobin concentration. We performed experiments on non-human primates during exsanguination to demonstrate that the limits of blood flow autoregulation can be accessed with NIRS.

Keywords: Near Infrared Spectroscopy, NIRS, Blood flow, Autoregulation, Hypotension, Brain

1. INTRODUCTION

The brain's ability to maintain a roughly constant cerebral blood flow (CBF) despite changes in cerebral perfusion pressure (CPP) is known as cerebral autoregulation (CA)¹. The effect is illustrated in Figure 1, known as Lassen's blood flow autoregulation curve, in which CBF remains approximately stable between the lower and upper limits of autoregulation (LLA & ULA).

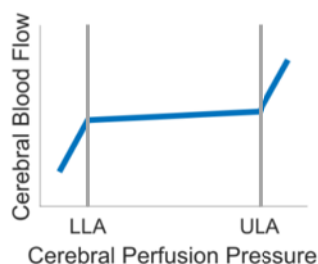


Figure 1: Simplified cerebral autoregulation curve by Lassen et. al¹. LLA and ULA determine the lower and upper limits of autoregulation, respectively. Between LLA and ULA the CA is intact and counteracts the influence of pressure changes.

Changes in intracranial pressure (ICP) or arterial blood pressure (ABP) will lead to changes in CPP, which is defined as the difference of ABP and ICP, and affects the transport of oxygen and nutrients to the cells if CA is impaired. Short periods of insufficient oxygen delivery can already lead to fainting, while long-term shortages lead to ischemia and in extreme cases causes ischemic strokes with potential fatal outcome². Dilation and constriction of blood vessel diameters is the brain's tool to control blood flow within a range of roughly $\pm 50\%$ of the normal CPP². In the case of intact CA, an increase in ABP (and therefore in CPP) is counteracted by a decrease in vessel diameter, which leads to a higher

resistance to the blood flow. If the increase in pressure and the degree of vessel diameter reduction are balanced, the net blood flow will remain stable. This CA mechanism is known as cerebrovascular or pressure reactivity. Contrarily, if CA is impaired, an increase in pressure will lead to an increase in blood flow; a decrease will cause a reduction and lead to deleterious effects. Because CA is known to be impaired during diseases like diabetes³, Parkinson's disease⁴, stroke⁵, traumatic brain injuries (TBI)⁶, hydrocephalus⁷, and others, methods for quantification are needed.

One way to quantify CA is to determine the limits of autoregulation and see if CPP is located on the regulated plateau part. To reconstruct Lassen's curve (Figure 1) CBF and CPP have to be measured. ICP and ABP can be measured directly via pressure sensors placed in the brain's ventricle and an A-line respectively. Since ICP sensors cannot be placed in many patients, Lassen's curve has also been reported using ABP alone. However, this is questionable when vascular reactivity is impaired. In contrast, cerebral blood flow is mostly indirectly measured. The currently most common method is transcranial Doppler sonography^{8,9}. It measures the cerebral blood flow velocity (CBFv) based on the movement of red blood cells. While it is non-invasive and has a high temporal resolution, it is only sensitive to large blood vessels, such as the middle cerebral artery. Therefore, a global autoregulation impairment state is captured, which is insensitive to local impairment. Transcranial Doppler sonography only captures the velocity of blood flow but cannot quantify the flow rate since the vessel diameter information is not available. In fact, the vessel diameter is assumed to be constant during these measurements², which disagrees with the theory of vascular reactivity.

Lassen's blood flow autoregulation curve has previously been derived from NIRS measured changes in tissue oxygen saturation (StO₂)¹⁰, where StO₂ was used as a surrogate for CBF. NIRS combines attractive features like non-invasiveness, high temporal resolution, sensitivity to microvasculature and localized measurements, making it suitable for low risk bedside monitoring. While StO₂ is influenced by CBF changes¹⁰, it is also dominated by cerebral blood volume (CBV). In order to decouple CBF and CBV influences in NIRS data, oxy- (HbO₂) and deoxy- (Hb) hemoglobin concentration changes need to be measured and interpreted by hemodynamic modeling¹¹⁻¹³. In order to address the need for disentangling CBF and CBV, we performed experiments on non-human primates during exsanguination. We will demonstrate that Lassen's curve and the lower limit of autoregulation can reliably be measured by NIRS.

2. METHODS

To understand the interplay between ICP, ABP, CPP and hemoglobin concentrations, an acute study on non-human primates (macaca mulatta, n=2) was performed. All experiments and procedures were approved by the University of Pittsburgh Institutional Animal Care and Use Committee (protocol ISO0005947). Animals were anesthetized on gas (1.5% isoflurane) during the experiment and ventilated by a respirator at 8 breaths/min. Body core temperature was held between 35 and 36 degrees Celsius. ABP was measured through an arterial line (A-line) in the external carotid artery by an ABP sensor (MPR 1 Datalogger, Raumedic, Germany). ICP was measured through a pressure sensor (NEUROVENT-P, Raumedic, Germany) in the ventricles. Both ABP and ICP data was collected with 100Hz sampling frequency. In addition, SpO₂ (peripheral arterial oxygen saturation measured with pulse oximetry on the monkey's foot), heart and respiration rate, etCO₂ (CO₂ at the end of exhaling) as well as core temperature were measured with a sampling frequency of 1Hz.

Cerebral hemoglobin concentrations were measured with a multi-distance, frequency domain NIRS system (OxiplexTS, ISS Inc., Champaign, IL, USA). The OxiplexTS system illuminates at two wavelengths (690nm and 830nm) of light. Data is recorded for four different source-detector distances, $d = 0.75\text{cm}$ to 2cm , which allows the calculation of absolute concentration of HbO₂ and Hb in local brain tissue using a multi-distance approach^{14,15}. Sampling frequency of the NIRS system was 5Hz. The NIRS probe was placed directly on the skull to avoid signal contamination from skin and muscle tissue. The probe was placed on the left hemisphere, approximately between frontal and parietal region. From the calculated Hb and HbO₂ values the total hemoglobin concentration ($\text{HbT} = \text{Hb} + \text{HbO}_2$) and the tissue oxygen saturation ($\text{StO}_2 = \text{HbO}_2/\text{HbT}$) were derived.

Exsanguination was performed to drain blood and thereby reduce ABP. Anesthesia via isoflurane was maintained throughout the procedure. At the time of exsanguination, the animals had been anesthetized for 9 hours, during which changes in ICP were induced (data not shown). At the time of exsanguination, ICP had been returned to normal levels. Exsanguination was started after infusion of 5ml heparin to stop blood coagulation. Drainage was performed through the A-line and was stopped intermittently to measure periods of ABP.

To compare pressure measurements and NIRS data, the data sampling frequency was equalized by down sampling the ABP and ICP to 5Hz. Down sampling was done by reading only every 20th data point. Since Lassen's autoregulation

curve is a static measure of autoregulation, only low frequency changes were considered. Therefore, a low pass filter with a cut-off frequency of 0.5Hz was applied. Since ABP measurements were not continuously measured during exsanguination, a 6th order polynomial fit was applied to the available data points to gain a continuous signal of mean arterial blood pressure (MAP). CPP was then calculated as the difference between filtered ICP and interpolated MAP. Lassen's blood flow autoregulation curve was recovered by averaging 10 seconds bins of NIRS derived signal and plotting the down sampled data over corresponding CPP bins.

3. RESULTS

We performed exsanguination in two non-human primates to lower blood pressure and obtain a NIRS derived surrogate for Lassen's blood flow autoregulation curve. The results can be seen in Figure 2, where Figure 2A shows the acquired measurements during exsanguination for one of the two animals. The gray, vertical dotted line marks the beginning of blood drainage. It can be seen that MAP and ICP both decrease over time, which also causes CPP to decrease. During arterial drainage, the HbO₂ concentration decreased, while Hb increases. However, HbO₂ is drained faster than Hb, which can be seen in the decreasing HbT trend, corresponding to the exsanguination. Tissue saturation, StO₂, followed decreasing trends of CPP. Data from the second animal (not shown) showed the same trends as reported in Figure 2A.

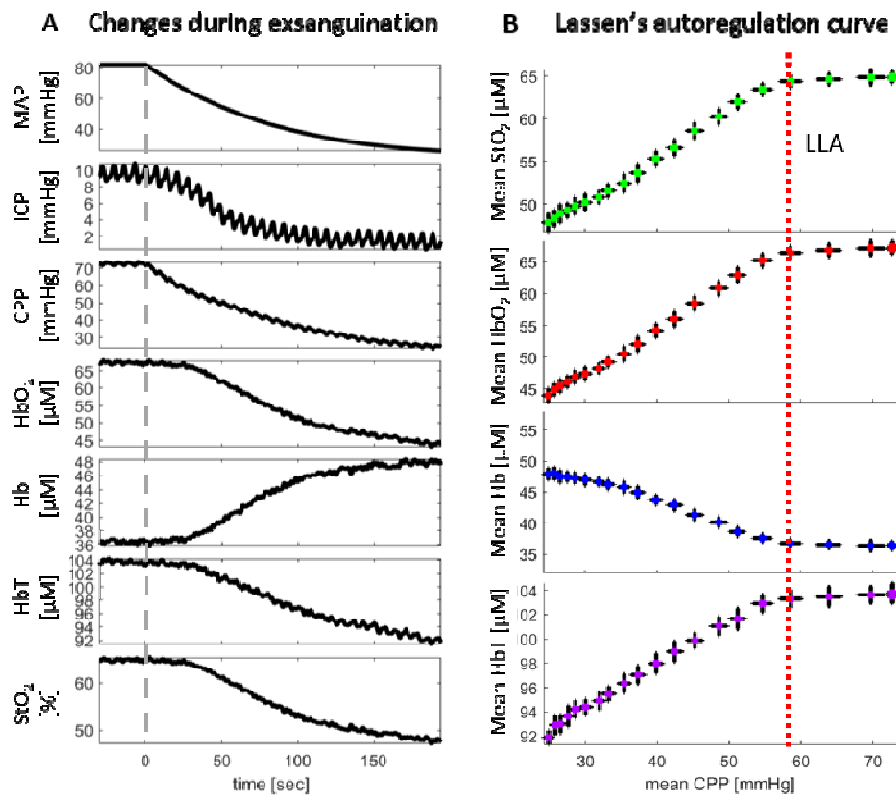


Figure 2: NIRS results during exsanguination. A) Time traces of pressure and hemodynamic measurements during exsanguination. ABP is represented as a fitted curve to short periods of measurements during blood drainage pauses. From the top: Mean arterial blood pressure (MAP), intracranial pressure (ICP), cerebral perfusion pressure (CPP), oxygenated hemoglobin (HbO₂), deoxygenated hemoglobin (Hb), total hemoglobin (HbT), and tissue oxygen saturation (StO₂). The dotted line marks the start of exsanguination. B) Reconstruction of Lassen's blood flow autoregulation curve with NIRS derived absolute hemoglobin concentrations. From the top: Tissue oxygen saturation (StO₂), oxygenated hemoglobin (HbO₂), deoxygenated hemoglobin (Hb), and total hemoglobin (HbT).

Lassen's autoregulation curve, using hemodynamic changes plotted against CPP, are seen in Figure 2B for averaged time bins of 10 seconds. The mean value of the time bin is shown as a colored dot while standard deviations in CPP and

NIRS measurements are given as black lines in horizontal and vertical direction, respectively. The figure reveals a distinct shape similar to the first half of Lassen's blood flow autoregulation curve (compare to Figure 1). The lower limit of autoregulation (LLA) is shown by the dotted line. While StO_2 , HbO_2 and HbT show the same general trend as seen in Figure 1, Hb increases with decreasing CPP. The data shown for animal 1 revealed a LLA of 65mmHg, animal 2 shows a LLA of 33mmHg.

We further calculated the slope of hemodynamic changes in Lassen's curves below the lower level of autoregulation. The difference in slopes for the not regulated part below the LLA is given in Table 1. Since HbT changes are directly related to CBV changes¹³, the slope of 0.34 $\mu M / mmHg$ corresponds to blood volume changes. On the other hand, HbO_2 , which is influenced by CBF and CBV, increases twice as fast as HbT .

Table 1: The slopes of Lassen's curves presented in Figure 2B for values below LLA

Variable	Slope
StO_2	0.52 [% / mmHg]
HbO_2	0.7 [$\mu M / mmHg$]
Hb	-0.35 [$\mu M / mmHg$]
HbT	0.34 [$\mu M / mmHg$]

4. DISCUSSION AND CONCLUSION

As shown in the results, reconstructing Lassen's blood flow autoregulation curve based on NIRS could be achieved. This leads to the conclusion that hemodynamic changes measured with NIRS is an alternative to blood flow measurements with other devices such as transcranial Doppler in order to quantify the limits of cerebral autoregulation.

The MAP level before exsanguination shown in Figure 2A Figure 1 lies at 80 mmHg and has to be considered hypertensive for non-human primates. A possible explanation for this might be chronic hypertension in MAP over previous years in the shown animal. ICP at 10mmHg represents a normal value for macaque and was artificially set. The resulting CPP before exsanguination is therefore elevated compared to animals with normal MAP. A relatively high amount of total hemoglobin concentration was also observed, with baseline HbT being 104 μM . Despite the high amount of HbT , the distribution of Hb and HbO_2 can be considered normal, shown by a StO_2 value of 65%. The second animal in this study (data not shown) had no known diseases and a normal MAP at 50mmHg, which results in a CPP of 40 mmHg before exsanguination.

Lassen's curve characteristics were reconstructed with all four available hemoglobin measurements as shown in Figure 2B. During arterial blood drainage HbO_2 and HbT concentration, as well as StO_2 , decreased as expected, while Hb increased. The same trend was found in the second animal (data not shown). Changes in HbO_2 are large compared to changes in Hb . This can also be observed by the slope of hemoglobin concentration over the same CPP range, which is significantly different between HbO_2 and Hb , as can be seen in Table 1. StO_2 and HbT are therefore not largely affected by increasing Hb . The other hemodynamic values StO_2 , HbT and HbO_2 show characteristics of the left side of Lassen's blood flow autoregulation curve.

A reason for the observed trend differences in Hb and HbO_2 might be given by the MAP reduction by blood drainage. The effects seen are likely caused by two different effects. The first is related to blood flow changes due to reduced MAP, the second part is a blood volume reduction primarily in the arteries that is not yet taken into account. In order to interpret the results in terms of Lassen's blood flow autoregulation curve, hemodynamic changes would need to be translated to CBF changes. A possible solution is the hemodynamic model introduced by Fantini et al.¹¹⁻¹³, which separates concentration changes in hemoglobin into blood flow velocity, blood volume and oxygen consumption related changes.

The ability of StO_2 to function as a surrogate for blood flow was previously mentioned by Brady et al.¹⁰, who reported the reconstruction of Lassen's blood flow autoregulation curve. In their study, a NIRS system was used to observe StO_2 on the frontal cortex during blood pressure hypotension induced in piglets. The hypotension was caused by slowly

inflating a balloon catheter in the inferior vena cava. StO_2 was then plotted over CPP to reconstruct Lassen's curve. However, the reconstruction was described as not well characterized, especially at the deflection points of LLA and ULA. Considering our results, the influence of blood volume changes by blocking the inferior vena cava might also have influenced the reliability of StO_2 as a surrogate for blood flow and the use of a hemodynamic modelling approach to disentangle volume and flow rate might benefit the outcome.

A modeling approach can address the ambiguity between CBF and CBV influence on NIRS data, which we will achieve with a modeling approach such as ¹¹⁻¹³. Separating blood volume and flow will allow for a more reliable NIRS based reconstruction of Lassen's curve and hence a better quantification of CA. In addition, the establishment of NIRS as a tool to monitor CA can be achieved.

REFERENCES

- [1] Lassen, N., "Cerebral blood flow and oxygen consumption in man.," *Physiol. Rev.* **39**(2), 183–238 (1959).
- [2] Payne, S., [Cerebral Autoregulation: Control of Blood Flow in the Brain], Springer International Publishing (2016).
- [3] Lundberg, N., "Continuous Recording and Control of Ventricular Fluid Pressure in Neurosurgical Practice.," *J. Neuropathol. Exp. Neurol.* **21**(3), 489, LWW (1962).
- [4] Vokatch, N., Gröttsch, H., Mermillod, B., Burkhard, P. R., Sztajzel, R., "Is cerebral autoregulation impaired in Parkinson's disease? A transcranial Doppler study," *J. Neurol. Sci.* **254**(1–2), 49–53 (2007).
- [5] Eames, P. J., Blake, M. J., Dawson, S. L., Panerai, R. B., Potter, J. F., "Dynamic cerebral autoregulation and beat to beat blood pressure control are impaired in acute ischaemic stroke.," *J. Neurol. Neurosurg. Psychiatry* **72**(4), 467–472 (2002).
- [6] Needham, E., McFadyen, C., Newcombe, V., Synnot, A., Czosnyka, M., Menon, D., "Cerebral Perfusion Pressure Targets Individualized to Pressure-Reactivity Index in Moderate to Severe Traumatic Brain Injury: A Systematic Review," *J. Neurotrauma* **8**, Epub ahead of print, Mary Ann Liebert, Inc., publishers (2016).
- [7] Momjian, S., Owler, B. K., Czosnyka, Z., Czosnyka, M., Pena, A., Pickard, J. D., "Pattern of white matter regional cerebral blood flow and autoregulation in normal pressure hydrocephalus," *Brain* **127**(5), 965–972, Oxford University Press (2004).
- [8] Panerai, R., "Assessment of cerebral pressure autoregulation in humans - a review of measurement methods," *Physiol Meas* **19**(3), 305–338 (1998).
- [9] Numan, T., Bain, A. R., Hoiland, R. L., Smirl, J. D., Lewis, N. C., Ainslie, P. N., "Static autoregulation in humans: a review and reanalysis," *Med. Eng. Phys.* **36**(11), 1487–1495, Institute of Physics and Engineering in Medicine (2014).
- [10] Brady, K. M., Lee, J. K., Kibler, K. K., Smielewski, P., Czosnyka, M., Easley, R. B., Koehler, R. C., Shaffner, D. H., "Continuous time-domain analysis of cerebrovascular autoregulation using near-infrared spectroscopy," *Stroke* **38**(10), 2818–2825 (2007).
- [11] Kainerstorfer, J. M., Sassaroli, A., Fantini, S., "Optical oximetry of volume-oscillating vascular compartments: contributions from oscillatory blood flow.," *J. Biomed. Opt.* **21**(10), 101408 (2016).
- [12] Kainerstorfer, J. M., Sassaroli, A., Hallacoglu, B., Pierro, M. L., Fantini, S., "Practical Steps for Applying a New Dynamic Model to Near-Infrared Spectroscopy Measurements of Hemodynamic Oscillations and Transient Changes. Implications for Cerebrovascular and Functional Brain Studies.," *Acad. Radiol.* **21**(2), 185–196, Elsevier Ltd (2014).
- [13] Fantini, S., "Dynamic model for the tissue concentration and oxygen saturation of hemoglobin in relation to blood volume, flow velocity, and oxygen consumption: Implications for functional neuroimaging and coherent hemodynamics spectroscopy (CHS)," *Neuroimage* **85**, 202–221, Elsevier Inc. (2014).
- [14] Fantini, S., Franceschini, M. A., Gratton, E., "Semi-infinite-geometry boundary problem for light migration in highly scattering media: a frequency-domain study in the diffusion approximation," *J. Opt. Soc. Am. B--OPTICAL Phys.* **11**(10), 2128 (1994).
- [15] Bigio, I. J., Fantini, S., [Quantitative Biomedical Optics: Theory, Methods, and Applications], 1st ed., Cambridge University Press, New York, NY, USA (2016).